Structural and Spectroscopic Evidence for Multiple α-Agostic Interactions in Dialkyl Complexes of Niobium

Andrew D. Poole,† David N. Williams,† Alan M. Kenwright,† Vernon C. Gibson,*,† William Clegg,‡ David C. R. Hockless,‡ and Paul A. O'Neil‡

Department of Chemistry, University Science Laboratories, South Road, Durham DH1 3LE, U.K., and Department of Chemistry, University of Newcastle, Newcastle upon Tyne, NE1 7RU, U.K.

Received March 29, 1993

Mono- and dineopentyl complexes of niobium containing ancillary imido and cyclopentadienyl ligands have been prepared via treatment of $(C_5H_5)Nb(NR)Cl_2$ (R = *t*-Bu, 2,6-C_6H_3-*i*-Pr_2) with 1 or 2 equiv of neopentylmagnesium chloride, respectively. The crystal structure of $(C_5H_5)Nb(N\text{-}2,6\text{-}C_6H_3\text{-}i\text{-}Pr_2)(CH_2CMe_3)_2$ ($C_{27}H_{43}NNb$, M_r = 474.6, monoclinic, $P2_1/n$, a = 9.272(1) Å, b = 17.237(2) Å, c = 17.020(2) Å, β = 95.02(1)°, V = 2709.7 Å^3, Z = 4, D_x = 1.163 g cm^{-3}, λ(Mo Kα) = 0.710 73 Å, μ = 0.44 mm^{-1}, $F(000)$ = 1012, T = 295 K) shows that a α-hydrogen on each neopentyl methylene lies within close contact (av 2.36 Å) of the metal center with Nb–C–H_α bond angles of 87 and 89°. The presence of α-agostic interactions is confirmed by NMR studies on the partially deuterated derivatives $(C_5H_5)Nb(NR)(CHDCMe_3)$ (R = *t*-Bu, 2,6-C_6H_3-*i*-Pr_2).

Introduction

Following the seminal contributions of Brookhart and Green,[1] interactions of alkyl ligand C–H bonds with coordinatively unsaturated transition metal centers have become well-established.[2] Multiple interactions of this type at a single metal center, however, remain relatively uncommon and are presently restricted to very low electron count transition metal complexes such as $(\eta\text{-}C_5Me_5)Ti(CH_2Ph)_3$[3] (formally 12 e$^-$) or complexes of the rare earth elements such as $(\eta\text{-}C_5Me_5)_2M(CH(SiMe_3)_2)$ (M = Y,[4] Nd[5]) and $(\eta\text{-}C_5Me_5)_2Th(CH_2CMe_3)_2$.[6] All of these examples have been characterized by diffraction techniques. In general, it is likely that many coordinatively unsaturated metal alkyls will possess agostic interactions of varying strengths and multiplicities depending upon the energies of the vacant metal orbitals and their steric accessibility. Herein, we report the solution- and solid-state characterization of some niobium alkyl complexes which possess two 3-center Nb–C–H interactions involving the α-C–H bonds of different alkyl ligands. The nature of the interactions in the solid state has been established by an X-ray structure determination, and they may be detected and differentiated in solution by NMR spectroscopy.

Scheme I

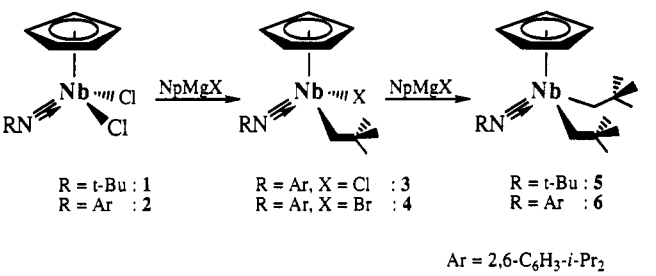

Synthesis

Mono- and dineopentyl complexes of niobium containing ancillary *tert*-butylimido and (2,6-diisopropylphenyl)-imido ligands may be prepared via treatment of the previously reported[7] dihalides **1** and **2** with neopentyl Grignard reagents (Scheme I).

Reaction of the dichloride **2** with 1 equiv of $BrMgCH_2CMe_3$ also results in halide exchange to afford the monobromo species $(C_5H_5)Nb(N\text{-}2,6\text{-}C_6H_3\text{-}i\text{-}Pr_2)(CH_2CMe_3)Br$ (**4**). **3** and **4** are red crystalline solids, moderately soluble in pentane, while **5** and **6** form pale yellow crystals which are exceedingly pentane soluble; crystals of **5** tend to be waxy at room temperature due to their low melting point (31–32 °C). Whereas **3** and **4** are stable indefinitely in hydrocarbon solution at ambient temperature, **5** and **6** decompose within hours via loss of neopentane to give black paramagnetic decomposition products presumably arising from an incipient neopentylidene species, which it has not proved possible to isolate or trap with a variety of reagents such as phosphines and unsaturated hydrocarbons.

† Department of Chemistry, University Science Laboratories, South Road, Durham DH1 3LE, U.K.

‡ Department of Chemistry, University of Newcastle, Newcastle upon Tyne, NE1 7RU, U.K.

(1) Brookhart, M.; Green, M. L. H. *J. Organomet. Chem.* **1983**, *250*, 395. Brookhart, M.; Whitesides, T. H.; Crockett, J. M. *Inorg. Chem.* **1976**, *15*, 1550. Lamanna, W.; Brookhart, M. *J. Am. Chem. Soc.* **1981**, *103*, 989. Brookhart, M.; Lamanna, W.; Humphrey, M. B. *J. Am. Chem. Soc.* **1982**, *104*, 2117. Schultz, A. J.; Teller, R. G.; Beno, M. A.; Williams, J. M.; Brookhart, M.; Lamanna, W.; Humphrey, H. B. *Science* **1983**, *220*, 197. Dawoodi, Z.; Green, M. L. H.; Mtetwa, V. S. B.; Prout, K. *J. Chem. Soc., Chem. Commun.* **1982**, 802. Dawoodi, Z.; Green, M. L. H.; Mtetwa, V. S. B.; Prout, K. *J. Chem. Soc., Chem. Commun.* **1982**, 1410. Dawoodi, Z.; Green, M. L. H.; Mtetwa, V. S. B.; Prout, K.; Schultz, A. J.; Williams, J. M.; Koetzle, T. F. *J. Chem. Soc., Dalton Trans.* **1986**, 1629.

(2) For recent comprehensive reviews, see: (a) Brookhart, M.; Green, M. L. H.; Wong, L. *Prog. Inorg. Chem.* **1988**, *36*, 1. (b) Crabtree, R. H.; Hamilton, D. G. *Adv. Organomet. Chem.* **1988**, *28*, 299.

(3) Mena, M.; Pellinghelli, M. A.; Royo, P.; Serrano, R.; Tiripicchio, A. *J. Chem. Soc., Chem. Commun.* **1986**, 1118.

(4) den Haan, K. H.; de Boer, L. J.; Teuben, J. H.; Spek, A. L.; Kojic-Prodic, B.; Hays, G. H.; Huis, R. *Organometallics* **1986**, *5*, 1726.

(5) Jeske, G.; Lauke, H.; Mauermann, H.; Swepston, P. N.; Schumann, H.; Marks, T. J. *J. Am. Chem. Soc.* **1985**, *107*, 8091.

(6) Bruno, J. W.; Smith, G. M.; Marks, T. J.; Fair, C. K.; Schultz, A. J.; Williams, J. M. *J. Am. Chem. Soc.* **1986**, *108*, 40.

(7) Williams, D. N.; Mitchell, J. P.; Poole, A. D.; Siemeling, U.; Clegg, W.; Hockless, D. C. R.; O'Neil, P. A.; Gibson, V. C. *J. Chem. Soc., Dalton Trans.* **1992**, 739.

0276-7333/93/2312-2549$04.00/0

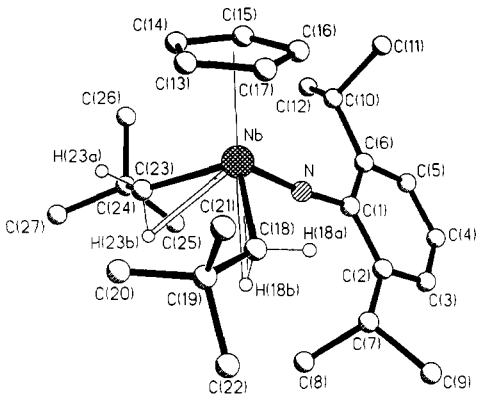

Figure 1. Molecular structure of **6** showing the atom labeling. H atoms are omitted except for neopentyl CH_2.

Table I. Crystal Data for 6

molecular formula	$C_{27}H_{43}NNb$
M	474.6
crystal system	monoclinic
crystal size (mm)	0.38 × 0.40 × 0.54
space group	$P2_1/n$
a (Å)	9.272(1)
b (Å)	17.237(2)
c (Å)	17.020(2)
β (deg)	95.02(1)
V (Å^3)	2709.7
Z	4
D_c (g cm^{-3})	1.163
F(000)	1012
μ (mm^{-1})	0.44
2θ range (deg)	3–50
max. indices h,k,l	11,20,20
no. of reflections measured	5275
no. of unique reflections	4760
no. of observed reflections	3476
R_{int}	0.019
transmission factors	0.74–0.78
weighting parameters	5, −15, 38, −12, 6, 17
parameters refined	304
max. shift (esd)	0.047
max. final electron density difference (e Å^{-3})	0.41
final R	0.0301
final R_w	0.0369
goodness of fit	1.03

The Molecular Structure of 6

The crystal structure of **6** has been determined and is shown in Figure 1. The crystal data are summarized in Table I, selected bond distances and angles are given in Table II, and atomic coordinates are collected in Table III. The imido ligand is close to linear (∠Nb–N–C = 174.6(2)°) with a Nb–N distance of 1.788(2) Å. This lies at the long end of the range found for niobium imido complexes (typically 1.73–1.79 Å[8]) and is significantly longer than the distance found in the starting dichloride **2** (1.761(6) Å[7]). Given the similar oxidation states of **2** and **6**, the longer Nb–N distance in **6** may in part reflect the lower electronegativity of the alkyl ligands compared with the chlorides of **2**, but the higher coordination number and different overall geometry of **6** undoubtedly also has a bearing on the Nb–N distance.

The cyclopentadienyl ring is bonded in η^5 fashion, although a significant ring-slip distortion is apparent, in accord with observations on other half-sandwich transition metal imido complexes.[7,9,10] A view of **6** through the Cp ring along the ring normal–metal vector is shown in Figure 2 and reveals that the metal is displaced in the direction of ring carbons C(15) and C(16) which are staggered with respect to the Nb–N bond; this contrasts with the structures of the dihalides in which the metal is displaced toward a ring carbon which eclipses the Nb–NR bond. The maximum deviation in metal to ring carbon distances is large, 0.161 Å, which compares with 0.120 Å for **2** and values ranging from 0.080 to 0.144 Å for analogous niobium

Table II. Selected Bond Lengths (Å) and Angles (deg) for 6

Nb–N	1.788(2)	Nb–C(13)	2.564(4)
Nb–C(14)	2.514(5)	Nb–C(15)	2.415(5)
Nb–C(16)	2.403(5)	Nb–C(17)	2.474(5)
Nb–X[a]	2.173(3)	Nb–C(18)	2.215(3)
Nb–C(23)	2.174(3)	Nb–H(18b)	2.405(33)
Nb–H(23b)	2.321(29)	N–C(1)	1.399(4)
C(13)–C(14)	1.402(7)	C(13)–C(17)	1.395(7)
C(14)–C(15)	1.377(7)	C(15)–C(16)	1.383(8)
C(16)–C(17)	1.402(8)		
X–Nb–N	124.3(1)	X–Nb–C(18)	112.9(2)
X–Nb–C(23)	112.5(2)	X–Nb–H(18b)	136.1(6)
X–Nb–H(23b)	130.9(6)	N–Nb–C(18)	97.9(1)
N–Nb–H(18b)	84.5(6)	N–Nb–C(23)	101.5(1)
N–Nb–H(23b)	97.0(9)	C(18)–Nb–H(18b)	23.5(7)
C(23)–Nb–H(23b)	24.3(8)	C(18)–Nb–C(23)	105.5(1)
H(18b)–Nb–H(23b)	65.1(11)	C(18)–Nb–H(23b)	82.6(8)
H(18b)–Nb–C(23)	89.4(7)	Nb–N–C(1)	174.6(2)
Nb–C(18)–C(19)	131.2(2)	Nb–C(18)–H(18b)	89.4(21)
Nb–C(18)–H(18a)	107.3(17)	H(18a)–C(18)–H(18b)	109.6(27)
Nb–C(23)–C(24)	132.5(3)	Nb–C(23)–H(23b)	86.5(17)
Nb–C(23)–H(23a)	107.0(20)	H(23a)–C(23)–H(23b)	105.3(32)

[a] X is the centroid of the Cp ring.

Table III. Fractional Atom Coordinates (×10^4) for 6

atom	x	y	z
Nb	1144.5(3)	1576.4(1)	2038.4(1)
N	597(2)	588(1)	1895(1)
C(1)	34(3)	−160(2)	1781(2)
C(2)	646(4)	−652(2)	1233(2)
C(3)	102(7)	−1410(2)	1149(3)
C(4)	−968(9)	−1666(3)	1572(3)
C(5)	−1554(7)	−1196(3)	2091(3)
C(6)	−1090(4)	−429(2)	2218(2)
C(7)	1838(4)	−367(2)	767(2)
C(8)	3312(6)	−415(3)	1229(3)
C(9)	1881(6)	−766(3)	−38(2)
C(10)	−1793(4)	88(3)	2780(2)
C(11)	−3262(5)	376(5)	2406(4)
C(12)	−1950(7)	−286(4)	3587(3)
C(13)	558(7)	3028(2)	2097(3)
C(14)	134(6)	2680(2)	2785(3)
C(15)	−936(5)	2146(3)	2576(3)
C(16)	−1205(5)	2152(3)	1763(3)
C(17)	−262(6)	2689(3)	1461(3)
C(18)	2436(3)	1682(2)	1009(2)
H(18a)	1819(32)	1530(20)	547(13)
H(18b)	3010(33)	1247(14)	1200(20)
C(19)	3520(4)	2308(2)	789(2)
C(20)	4432(7)	2582(4)	1510(4)
C(21)	2761(6)	2986(3)	367(3)
C(22)	4508(6)	1933(4)	218(4)
C(23)	2715(4)	1480(2)	3059(2)
H(23a)	2987(40)	1997(10)	3215(22)
H(23b)	3396(32)	1327(22)	2696(18)
C(24)	2748(4)	994(2)	3817(2)
C(25)	2623(6)	145(2)	3621(3)
C(26)	1523(7)	1234(4)	4286(3)
C(27)	4184(6)	1127(3)	4314(3)

(8) Cotton, F. A.; Duraj, S. A.; Roth, W. J. *J. Am. Chem. Soc.* **1984**, *106*, 4749. Finn, P. A.; King, M. S.; Kitty, P. A.; McCarley, R. E. *J. Am. Chem. Soc.* **1975**, *97*, 220. Tan, L. S.; Goeden, G. V.; Haymore, B. L. *Inorg. Chem.* **1983**, *22*, 1744.

(9) Green, M. L. H.; Konidaris, P. C.; Mountford, P.; Simpson, S. J. *J. Chem. Soc., Chem. Commun.* **1992**, 256.

(10) Herrmann, W. A.; Weichselbaumer, G.; Paciello, R. A.; Fischer, R. A.; Herdtweck, E.; Okuda, J.; Marz, D. W. *Organometallics* **1990**, *9*, 489.

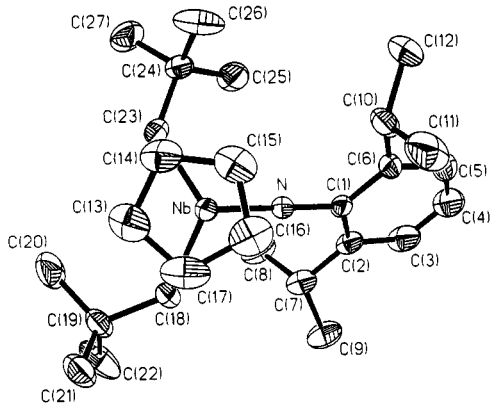

Figure 2. View of **6** along the normal to the Cp ring with thermal ellipsoids at 25% probability level. H atoms omitted.

dihalides reported to date.[7] A good measure of ring slippage is provided by the distance between the C_5H_5 ring centroid and the point where the Nb–C_5H_5 ring normal meets the "best plane" for the C_5H_5 ring (the slip vector[11]). This is 0.174 Å for **6**, which compares with a value of 0.048 Å for **2**. The deviations in the inter-ring carbon distances, however, are not sufficiently pronounced (e.g. the maximum deviation of inter-ring carbon distances for **6** is 0.025 Å, compared with 0.119 Å for **2**) to support a generalized (e.g. allyl-ene) description of the ring distortion.

Two hydrogens, one on each of the two neopentyl methylene units, lie in close contact (av 2.36 Å) with the metal center giving rise to Nb–C–H_α angles of 87 and 89° (see Figure 1). These C–H bonds were restrained in length during the structure refinement but their directions were refined freely. The Nb–C(23) and Nb–H(23b) distances, at 2.174(3) and 2.321(29) Å, are shorter than the corresponding Nb–C(18) and Nb–H(18b) distances [2.215(3) and 2.405(33) Å, respectively], indicating that the former is the stronger agostic interaction. The C(23)–H(23b) bond lies close to the plane containing the metal and the two neopentyl methylene carbons; the angle between the planes defined by Nb–C(23)–H(23b) and Nb–C(18)–C(23) is 20.1°, while the angle between Nb–C(18)–H(18b) and Nb–C(18)–C(23) is 48.3°. The ring centroid–Nb–C_α angles are identical [112.7(2)° (av)] within experimental error.

Spectroscopic Studies

The agostic interactions can be observed by infrared and NMR spectroscopies. The infrared spectrum, recorded on *neat* **5** between CsI plates, revealed a broad absorption at 2700 cm^{-1} attributable to the bridging C–H stretch. Unfortunately, a spectrum on the dideuterio derivative $(C_5H_5)Nb(N\text{-}t\text{-}Bu)(CHDCMe_3)_2$ (**5**-d_2) gave a number of broad, weak absorptions in the region expected for the C–D absorption, and therefore we were unable to assign the agostic C–D stretch without ambiguity.

In the ^1H NMR spectrum of **5**, the diastereotopic methylene hydrogens of the neopentyl ligands occur at δ 2.31 and −0.20 ppm[12] (Table IV, Figure 3a), and both possess C–H coupling constants of 112 Hz,[13] consistent with the average of a "normal" sp^3 C–H coupling and the C–H coupling of a 3-center M–C–H (agostic) interaction, although here care has to be exercised in the use of α-C–H

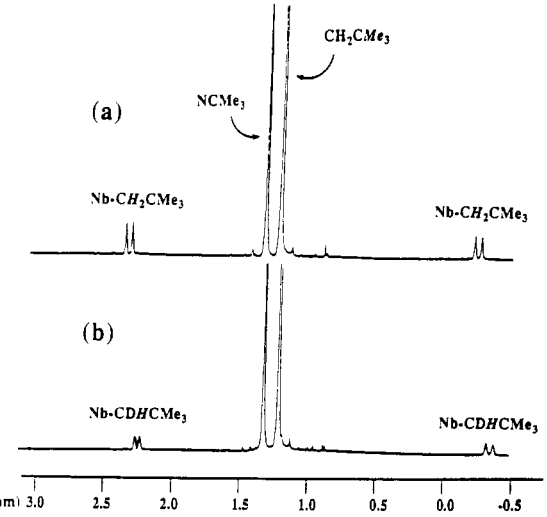

Figure 3. 250-MHz ^1H NMR spectra (C_6D_6) of the alkyl region of (a) per-protio **5**, and (b) **5**-d_2 at room temperature (vertical scales nonidentical).

coupling constants as a criterion for determining the presence of α-agostic interactions due to the effect of the metal and its ancillary ligands on the hybridization of the metal-bound carbon.[14] Difference NOE experiments[15] between each methylene resonance and the C_5H_5 and *tert*-butyl groups of the imido ligand in **5** indicate that the methylene hydrogens giving rise to the higher field signal are, on average, orientated toward the Cp ring, while its diastereotopic partner is directed toward the imido ligand. The ^1H NMR spectrum of **6** shows essentially the same features except the low-field methylene region is complicated by the presence of overlapping resonances due to the isopropyl methyl substituents of the 2,6-N-C_6H_3-*i*-Pr_2 ligand; for this reason, the subsequent discussion of the NMR data will be restricted to **5**, although the same series of experiments were also conducted on **6** to ensure that each compound behaved in an analogous manner. From the crystal data on **6**, it can be seen that H_{23a} lies closest to the Cp ring and the proton resonance for this hydrogen will be averaged with that for H_{18b} via rotation about the Nb–C bonds. This can be seen more clearly from the idealized view below (where H_1 and H_2 correspond to H_{23a} and H_{18b} in the molecular structure shown in Figure 1; the imido ligand is not shown for reasons of clarity but would project to the rear of the molecule as viewed).

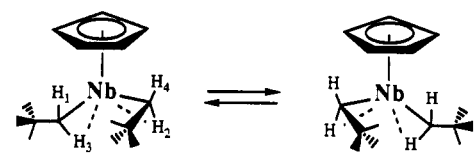

(11) Faller, J. W.; Crabtree, R. H.; Habib, A. *Organometallics* **1985**, *4*, 929.

(12) In general, the chemical shifts of the bridging hydrogens in d^0 alkyls are not a reliable indicator of M–C–H interactions.

(13) Determined from the ^1H NMR spectrum due to ^{93}Nb quadrupolar broadening of the α carbon ^{13}C resonances. The only other Nb–neopentyl complex for which a $J(C_\alpha\text{–}H)$ coupling constant has been reported is $Nb(CHCMe_3)(CH_2CMe_3)_3$ with a value of 101 Hz. [Schrock, R. R.; Fellman, J. D. *J. Am. Chem. Soc.* **1978**, *100*, 3359.] Related tantalum compounds are found to possess values over a considerable range (110–121 Hz) [Fellman, J. D.; Schrock, R. R.; Traficante, D. D. *Organometallics* **1982**, *1*, 481] which may or may not be indicative of agostic interactions of differing strengths.

(14) Finch, W. C.; Anslyn, E. V.; Grubbs, R. H. *J. Am. Chem. Soc.* **1988**, *110*, 2406.

(15) Irradiation of the C_5H_5 resonance leads to a positive NOE on the signal at δ −0.20 ppm but has negligible effect on the δ 2.31 ppm resonance; conversely, irradiation of the *tert*-butyl resonance at δ 1.32 ppm shows a positive NOE to the signal at δ 2.31 ppm but no effect on the resonance at δ −0.20 ppm.

Table IV. NMR Data

compound	assignment	chemical shifts (ppm), multiplicity, coupling consts (Hz) ^{1}H[a]	^{13}C[b]
$(C_5H_5)Nb(N\text{-}2,6\text{-}C_6H_3\text{-}i\text{-}Pr_2)(CH_2CMe_3)Cl$ (**3**)[c]	*m*-C_6H_3	7.06, d, ^3J(HH) = 7.5	123.1, d, ^1J(CH) = 156
	p-C_6H_3	6.95, t, ^3J(HH) = 7.5	125.4, d, ^1J(CH) = 160
	C_5H_5	5.74, s	110.5, d, ^1J(CH) = 175
	$CH(CH_3)_2$	3.99, sept, ^3J(HH) = 7.5	28.1, d, ^1J(CH) = 127
	$CH_2C(CH_3)_3$	2.46, d, ^2J(HH) = 12.5, ^1J(CH) = 123 1.64, d, ^2J(HH) = 12.5	86.3, br ($\nu_{1/2}$ = 33 Hz)[d]
	$CH(CH_3)_2$	1.18, d, ^3J(HH) = 7.5	24.0, q, ^1J(CH) = 126 24.8, q, ^1J(CH) = 126
	$CH_2C(CH_3)_3$	1.15, s	34.6, q, ^1J(CH) = 124
	$CH_2C(CH_3)_3$		36.3, s
	o-C_6H_3		145.7, s
	ipso-C_6H_3		151.8, s
$(C_5H_5)Nb(N\text{-}2,6\text{-}C_6H_3\text{-}i\text{-}Pr_2)(CH_2CMe_3)Br$ (**4**)	*m*-C_6H_3	7.06, d, ^3J(HH) = 7.6	123.2, d, ^1J(CH) = 156
	p-C_6H_3	6.96, *t*, ^3J(HH) = 7.6	125.5, d, ^1J(CH) = 160
	C_5H_5	5.76, s	110.3, d, ^1J(CH) = 176
	$CH(CH_3)_2$	4.06, sept, ^3J(HH) = 6.8	27.9, d, ^1J(CH) = 125
	$CH_2C(CH_3)_3$	2.54, d, ^2J(HH) = 11.6, ^1J(CH) = 123 1.34, d, ^2J(HH) = 11.6	92.1, br ($\nu_{1/2}$ = 63 Hz)[d]
	$CH(CH_3)_2$	1.31, d, ^3J(HH) = 6.8	23.7, q, ^1J(CH) = 126 24.6, q, ^1J(CH) = 126
	$CH_2C(CH_3)_3$	1.12, s	33.2, q, ^1J(CH) = 125
	$CH_2C(CH_3)_3$		36.7, s
	o-C_6H_3		145.2, s
	ipso-C_6H_3		151.6, s
$(C_5H_5)Nb(N\text{-}t\text{-}Bu)(CH_2CMe_3)_2$ (**5**)[c]	C_5H_5	5.68, s	106.4, d, ^1J(CH) = 173
	$CH_2C(CH_3)_3$	2.31, d, ^2J(HH) = 11.4, ^1J(CH) = 112	81.2
	$NC(CH_3)_3$	1.32, s	32.8, q, ^1J(CH) = 126
	$CH_2C(CH_3)_3$	1.28, s	34.5, q, ^1J(CH) = 124
	$CH_2C(CH_3)_3$	–0.20, d, ^2J(HH) = 11.4, ^1J(CH) = 112	81.2, br
	$CH_2C(CH_3)_3$		34.8, s
	$NC(CH_3)_3$		65.6, s
$(C_5H_5)Nb(N\text{-}t\text{-}Bu)(CHDCMe_3)_2$ (**5**-d_2)	C_5H_5	5.68, s	
	$CHDC(CH_3)_3$	2.25 (br), 2.21 (br) –0.25 (br), –0.30 (br)	
	$NC(CH_3)_3$	1.32, s	
	$CHDC(CH_3)_3$	1.22, s	
$(C_5H_5)Nb(N\text{-}2,6\text{-}C_6H_3\text{-}i\text{-}Pr_2)(CH_2CMe_3)_2$ (**6**)[c]	*m*-C_6H_3	7.10, d, ^3J(HH) = 5.0	123.0, d, ^1J(CH) = 155
	p-C_6H_3	6.98, t, ^3J(HH) = 5.0	123.9, d, ^1J(CH) = 159
	C_5H_5	5.86, s	107.4, d, ^1J(CH) = 174
	$CH(CH_3)_2$	4.08, sept, ^3J(HH) = 7.5	27.9, d, ^1J(CH) = 128
	$CH(CH_3)_2$	1.32, d, ^3J(HH) = 7.5	24.5, q, ^1J(CH) = 125
	$CH_2C(CH_3)_3$	1.88, d, ^2J(HH) = 11.8, ^1J(CH) = 113 1.12, d, ^2J(HH) = 11.8	85.7, br
	$CH_2C(CH_3)_3$	1.12, s	34.3, q, ^1J(CH) = 125
	$CH_2C(CH_3)_3$		36.4, s
	o-C_6H_3		145.1, s
	ipso-C_6H_3		152.2, s
$(C_5H_5)Nb(N\text{-}2,6\text{-}C_6H_3\text{-}i\text{-}Pr_2)(CHDCMe_3)_2$ (**6**-d_2)	*m*-C_6H_3	7.10, d, ^3J(HH) = 5.0	
	p-C_6H_3	6.98, t, ^3J(HH) = 5.0	
	C_5H_5	5.87, s	
	$CH(CH_3)_2$	4.06, sept, ^3J(HH) = 7.5	
	$CH(CH_3)_2$	1.32, d, ^3J(HH) = 7.5	
	$CHDC(CH_3)_3$	1.82 (br)[e], 1.77 (br), 1.06 (br)[e], 1.02 (br)[e]	
	$CH_2C(CH_3)_3$	1.11, s	

[a] Recorded at 399.95 MHz in C_6D_6 unless otherwise stated. [b] Recorded at 100.58 MHz in C_6D_6 unless otherwise stated. [c] ^{1}H NMR recorded at 250.13 MHz. [d] Resonance broadened due to proximity to ^{93}Nb quadrupole nucleus. [e] Resonances partially obscured by other signals; shifts estimated.

Thus, on the basis of the NOE measurements, the high-field signal can be assigned with some confidence to $(H_1/H_2)_{av}$ with an averaged $^2J_{HH}$ of 11.4 Hz while the low-field doublet resonance is attributable to $(H_3/H_4)_{av}$. It can also be seen from the view above that H_2 and H_3 are the protons lying in close contact with the metal center (indicated by dashed lines).

In order to confirm the presence of the agostic interactions, the partially deuterated compounds $(\eta\text{-}C_5H_5)Nb(NR)(CHDCMe_3)_2$ (R = *t*-Bu, **5**-d_2; 2,6-C_6H_3-*i*-Pr_2, **6**-d_2) were prepared via treatment of **1** and **2** with excess BrMg(CHDCMe$_3$). The ^{1}H NMR spectrum of **5**-d_2 is shown in Figure 3b. It can be seen that the methylene resonances for per-protio **5** are replaced by four broadened signals, all shifted to higher field and each integrating as $^1/_2$ proton. These are four distinct signals rather than two doublets, and their assignment as methylene protons geminal to deuterons was confirmed by deuterium decoupling experiments. The four signals arise due to the four possible diastereoisomers[16] shown in Figure 4.

It is also clear that one of the resonances in each pair experiences a greater upfield shift (0.11 ppm relative to the per-protio compound), consistent with the presence of agostic interactions in both the H_1/H_2 and H_3/H_4

(16) *R,S* assignments have been made according to the Baird–Sloan modification of the Cahn–Ingold–Prelog priority rules: ^{93}Nb > *t*-Bu > D > H. (Stanley, K.; Baird, M. C. *J. Am. Chem. Soc.* **1975**, 97, 6598. Sloan, T. E. *Top. Stereochem.* **1981**, 12, 1.)

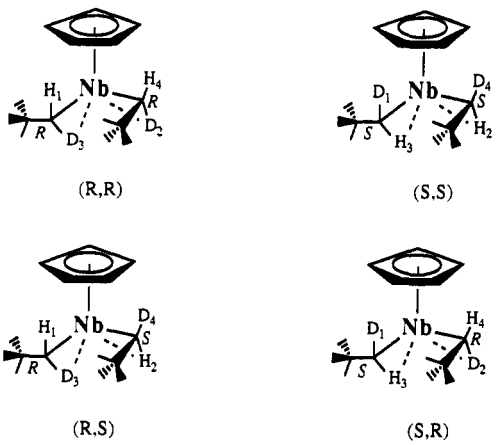

Figure 4. Diastereoisomers of $(C_5H_5)Nb(N\text{-}t\text{-}Bu)(CHDCMe_3)_2$. The N-*t*-Bu ligand, omitted for clarity, projects to the rear of the molecule as viewed.

interchanging pairs. This is in accord with the solid-state structure which shows that the agostic interactions occur for H_2 and H_3.[17] On the other hand, the lower field resonances of each pair are shifted by *ca.* 0.06 ppm, which is more consistent with simple isotopic substitution of a nonagostic C–H bond bound to an electropositive metal.[18] These observations may be understood by considering the exchange between agostic and nonagostic sites for each stereoisomer (Figure 5). It is only for the enantiomeric (*S,S*) and (*R,R*) pair that exchange of H_1 and H_2 between agostic and nonagostic sites can occur, and therefore it is only for these isomers that isotopic perturbation of resonances is expected and indeed observed. Therefore, the resonances, in decreasing order of chemical shift, may be assigned as $(H_3/H_4)_{av}$ for *S,R*; $(H_3/H_4)_{av}$ for the *S,S*/*R,R* pair; $(H_1/H_2)_{av}$ for *R,S*; $(H_1/H_2)_{av}$ for the *S,S*/*R,R* pair.

There is also a marked temperature dependence of the chemical shifts of the methylene resonances (Figure 6). The two high-field signals for **5**-d_2 ($CDCl_3$)[19] shift from δ −0.38 (*R,S*) and −0.34 ppm (*S,S*/*R,R*) at +40 °C to δ −0.62 and −0.56 ppm, respectively, upon cooling to −50 °C. The temperature dependence of the chemical shift for the *R,S* resonance closely shadows the shift change for the methylene doublet resonance of the per-protio compound (the chemical shift difference between the two resonances remaining constant at ca. 0.06 ppm), whereas the upfield *S,S*/*R,R* resonance shifts to a greater extent, consistent with an isotopic perturbation of resonance effect for this signal; the enhanced separation of the two signals at −50 °C is clearly evident in Figure 6. A similar effect is observed for the lower field resonances which move from δ 2.16 and 2.19 ppm to δ 2.24 and 2.29 ppm, respectively. However, the *downfield* shift of these resonances upon cooling is in the *opposite* direction to the movement observed in the room temperature ^1H NMR spectrum for **5**-d_2 relative to

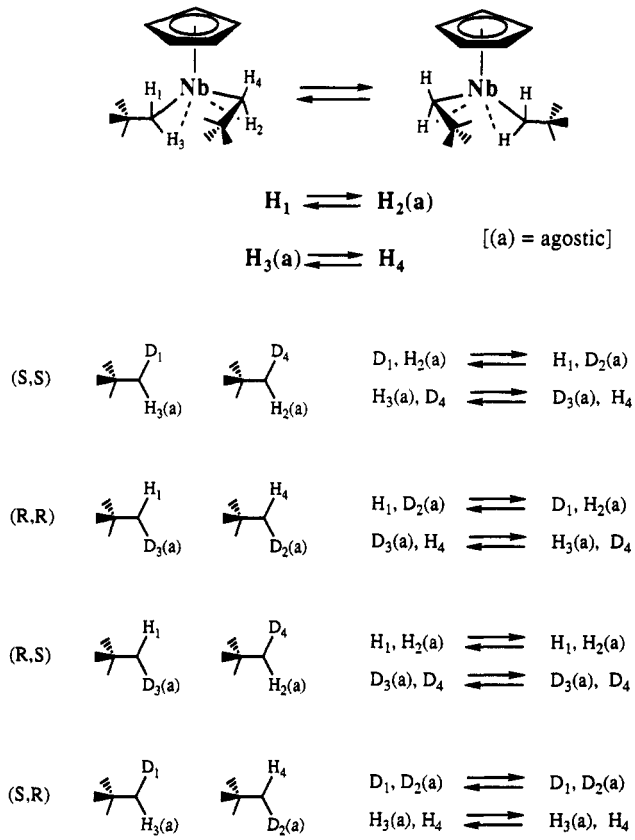

Figure 5. Scheme showing the interchange of the methylene H/D sites resulting from rotation about the Nb–C bonds of the neopentyl ligands.

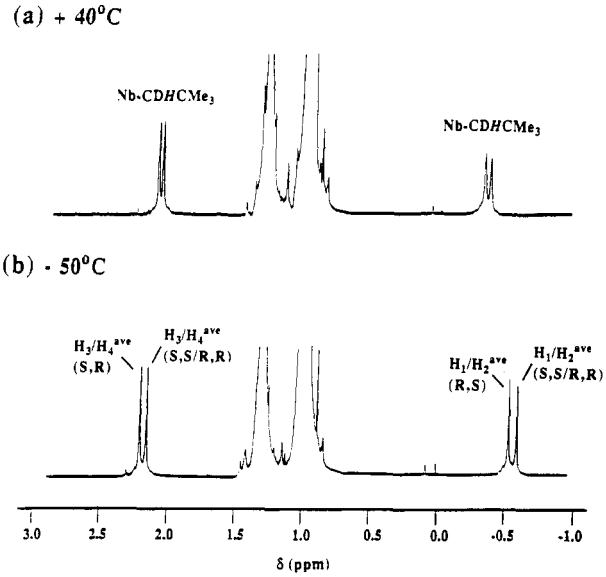

Figure 6. 400-MHz ^1H NMR spectra ($CDCl_3$) of the alkyl region of **5**-d_2 (a) at +40 °C and (b) at −50 °C (vertical scales greatly expanded).

the per-protio compound (Figure 3). It is an intriguing possibility that this could reflect a strengthening of the M–C–H interaction for one of the methylene orientations at the expense of the agostic interaction for the other. Such an effect would not necessarily be surprising since the accessibilities of the different metal acceptor orbitals may change as the temperature is lowered.

Discussion and Summary

The presence of two agostic interactions in **6** is at first a little surprising and poses an intriguing question as to

(17) The solid-state structure would correspond to the (*S,S*) isomer if the deuteriums were to be placed in the energetically preferred terminal sites.

(18) The "normal" isotopic shift for a *n*-alkane is *ca.* 0.02 ppm, e.g. 0.019 for CH_3D. However, the isotope shift for protons attached to more electronegative elements is usually larger, e.g. 0.03 for HDO; it is, therefore, expected that the shift for CH(D) units attached to an electropositive metal such as niobium will be somewhat larger than normal due to the substantial $Nb^{\delta+}$–$C^{\delta-}$ polarization. See: Lambert, J. B.; Greifenstein, L. G. *J. Am. Chem. Soc.* **1974**, *96*, 5120. Bernheim, R. A.; Batiz-Hernandez, H. *J. Chem. Phys.* **1966**, *45*, 2261.

(19) The variable-temperature ^1H NMR experiment is reported in chloroform-d_1 due to fortuitous overlap of the toluene methyl resonance (2.09 ppm) with the low-field methylene signal. The same qualitative temperature dependence is observed, however, in toluene solution.

the electron count of this complex. Agostic interactions excluded, **6** is formally a 16-electron species. However, addition of four more electrons from the two agostic C–H bonds (considered to interact with a metal via donation of the C–H bonding pair of electrons) would then give a 20-electron complex. The actual situation may, however, lie somewhere in between these two extremes. For example, the crystal structure shows a substantial distortion of the C_5H_5 ring, which is often found when a cyclopentadienyl ring is in direct competition with an imido group for available metal d_π symmetry orbitals.[7,9,10] While the distortion cannot be regarded as a complete adjustment to an η^3-C_5H_5 coordination mode, it may nonetheless be attributed to back donation of electron density from the metal center into the empty δ symmetry orbitals on the Cp ring, thus alleviating the build up of electron density at the metal. It is also worth considering the consequences of the similarities between the frontier orbitals of the half-sandwich imido fragment [CpNb(NR)][7] and those of bent metallocenes.[20] For the latter, it has been shown that metal–ligand interactions outside the normal metallocene "equatorial" binding plane lead to destabilization of metal–C_5H_5 ring bonding interactions. Since one of the agostic interactions [C(18)–H(18b)] clearly lies out of the metallocene binding plane, there is also likely to be an effect on metal–ring bonding through a competition with the agostic interaction. We also noted that the Nb–N bond distance is somewhat lengthened compared with the formally 16-electron starting dichloride; although the agostic interactions would not normally be expected to compete effectively with an imido ligand for metal orbitals, they serve to increase the coordination number of the metal and also augment the "electronic pressure" at the metal.

The presence of agostic interactions also provides an attractive explanation for the instability of **5** and **6** to loss of neopentane. If the decomposition proceeds via a metal-mediated α-hydrogen abstraction pathway, the reaction would be expected to be facilitated by the agostic interactions already present in the complex. This contrasts with the situation found for the bis-benzyl analogue (C_5Me_5)Nb(N-2,6-C_6H_3-*i*-Pr_2)($CH_2Ph)_2$ which is stable to >100 °C in the absence of base but reacts with PMe_3 at ca. 60 °C to give the thermally robust benzylidene complex Cp*Nb(NAr)(CHPh)(PMe_3).[21]

In summary, these studies have shown that multiple α-agostic interactions can occur at a coordinatively unsaturated metal center, and given a suitable combination of ligands and partial deuteration of the agostic sites, they may be readily detected and differentiated in solution by NMR spectroscopy.

Experimental Section

General Considerations. All manipulations were performed on a conventional vacuum/inert atmosphere line using standard Schlenk and cannula techniques or in a dry inert atmosphere glovebox. The following solvents were dried by prolonged refluxing over a suitable drying agent and were freshly distilled and deoxygenated prior to use (drying agent in parentheses): toluene (sodium metal), *n*-pentane (lithium aluminum hydride), diethyl ether (lithium aluminum hydride). Benzene-d_6, toluene-d_8, and chloroform-d_1 were dried by vacuum distillation from phosphorus(V) oxide and stored over activated 4-Å molecular sieves. Elemental analyses were performed by the microanalytical services of this department. Mass spectra were recorded on a VG 7070E mass spectrometer. Infrared spectra were recorded on Perkin-Elmer 577 and 457 grating spectrophotometers by using either KBr or CsI windows. Absorptions are abbreviated as s (strong), m (medium), w (weak), br (broad), sp (sharp), sh (shoulder). NMR spectra were recorded on the following instruments, at the frequencies listed: Bruker AC 250, ^1H (250.13 MHz), ^{13}C (62.90 MHz); Varian VXR400, ^1H (399.95 MHz), ^{13}C (100.58 MHz). The following abbreviations have been used for band multiplicities: s (singlet), d (doublet), t (triplet), q (quartet), qnt (quintet), sept (septet), m (multiplet). Chemical shifts are quoted to the following references, unless stated otherwise: ^{13}C (C_6D_6, 128.0 ppm); ^1H (C_6D_6, 7.15 ppm); ^1H ($CDCl_3$, 7.24 ppm). (C_5H_5)Nb(N-*t*-Bu)Cl_2,[7] (C_5H_5)Nb(N-2,6-C_6H_3-*i*-Pr_2)Cl_2[7], $ClMgCH_2CMe_3$, and $BrMgCHDCMe_3$[22] were prepared according to previously published procedures.

Synthesis of (C_5H_5)Nb(N-2,6-C_6H_3-*i*-Pr_2)(CH_2CMe_3)Cl (3). To a stirred solution of (C_5H_5)Nb(N-2,6-C_6H_3-*i*-Pr_2)Cl_2 (**2**) (1.0 g, 2.48 mmol) in diethyl ether (50 mL) at −78 °C was added via syringe a diethyl ether solution of $ClMg(CH_2CMe_3)$ (2.48 mmol). The mixture was warmed to room temperature and stirred for 2 h to give an orange-brown solution which was filtered from the $MgCl_2$ residue. After removal of the solvent under reduced pressure, an oily orange-red solid remained. This was washed with cold *n*-pentane (2 × 5 mL), and the residue was recrystallized from a concentrated *n*-pentane solution at −78 °C to yield red crystals. Yield: 0.59 g, 54%. Anal. Calcd for $C_{22}H_{33}NNbCl$: C, 60.1; H, 7.6; N, 3.2. Anal. Found: C, 60.0, H, 7.8; N, 3.1. MS (EI): $[M - Cl - CH_2CMe_3]^+$ 369. IR (CsI, cm^{-1}): 3010 (w), 2910 (s), 2860 (s), 1460 (s), 1440 (m), 1380 (m), 1360 (m), 1330 (s), 1290 (s), 1230 (w), 1100 (br), 1020 (br), 980 (m), 760 (s), 460 (s), 380 (m), 360 (m).

Synthesis of (C_5H_5)Nb(N-2,6-C_6H_3-*i*-Pr_2)(CH_2CMe_3)Br (4). (C_5H_5)Nb(N-2,6-C_6H_3-*i*-Pr_2)(CH_2CMe_3)Br (**4**) was prepared by an analogous procedure to that described for (C_5H_5)Nb(N-2,6-C_6H_3-*i*-Pr_2)(CH_2CMe_3)Cl (**3**), via the reaction of (C_5H_5)Nb(N-2,6-C_6H_3-*i*-Pr_2)Cl_2 (**2**), (1.0 g, 2.48 mmol), with $BrMgCH_2CMe_3$ (2.48 mmol). Yield: 0.42 g, 35%. Anal. Calcd for $C_{22}H_{33}NNbBr$: C, 54.5; H, 7.1; N, 3.1. Found: C, 54.7; H, 7.5; N, 3.1. MS (EI): $[M]^+$ 485. IR (CsI, cm^{-1}): 2910 (s), 2840 (s), 1720 (w), 1460 (s), 1380 (m), 1365 (m), 1330 (m), 1285 (m), 1230 (w), 1100 (br), 1020 (w), 975 (w), 805 (m), 750 (s), 730 (m), 720 (m), 450 (br), 375 (br).

Synthesis of (C_5H_5)Nb(N-*t*-Bu)($CH_2CMe_3)_2$ (5). To a stirred solution of (C_5H_5)Nb(N-*t*-Bu)Cl_2 (**1**) (0.5 g, 1.67 mmol) in diethyl ether (20 mL) at −78 °C was added a diethyl ether solution of $ClMgCH_2CMe_3$ (3.42 mmol). The mixture was allowed to warm to room temperature and stirred for a further 6 h. The supernatant solution was then filtered from the $MgCl_2$ residue and the solvent removed under reduced pressure to afford a red-brown oil. The oil was extracted into *n*-pentane (10 mL) and cooled to −78 °C to give pale yellow crystals. Yield: 0.45 g, 73%. Anal. Calcd for $C_{19}H_{36}NNb$: C, 61.4; H, 9.8; N, 3.8; Nb, 25.0. Found: C, 61.1; H, 9.6; N, 3.4; Nb, 24.7. MS (CI): $[M + C_5H_{12}]^+$ 446, $[M + C_3H_8]^+$ 414. IR (CsI, cm^{-1}): 3010 (w, sh), 2700 (w, br), 1460 (m), 1445 (m, sh), 1375 (w, sh), 1358 (s), 1242 (vs), 1129 (w), 1018 (m), 810 (vs), 799 (vs), 754 (w), 580 (w), 532 (w), 520 (w), 368 (w).

Synthesis of (C_5H_5)Nb(N-*t*-Bu)($CHDCMe_3)_2$ (5-d_2). An analogous procedure was adopted to that described for (C_5H_5)Nb(N-*t*-Bu)($CH_2CMe_3)_2$ (**5**).

Synthesis of (C_5H_5)Nb(N-2,6-C_6H_3-*i*-Pr_2)($CH_2CMe_3)_2$ (6). (C_5H_5)Nb(N-2,6-C_6H_3-*i*-Pr_2)($CH_2CMe_3)_2$ (**6**) was prepared by an analogous procedure to that described for (C_5H_5)Nb(N-*t*-Bu)($CH_2CMe_3)_2$ (**5**), via the reaction of (C_5H_5)Nb(N-2,6-C_6H_3-*i*-Pr_2)Cl_2 (**2**) (1.0 g, 2.48 mmol) with $ClMgCH_2CMe_3$ (9.92 mmol). Yield: 0.62 g, 53%. Anal. Calcd for $C_{27}H_{44}NNb$: C, 68.2; H, 9.3; N, 2.9. Found: C, 68.1; H, 9.6; N, 2.6. MS (EI): $[M - 2(CH_2CMe_3)]^+$ 330. IR (CsI, cm^{-1}): 3060 (w), 2910 (s), 2850 (s), 2700 (br), 1460

(20) Lauher, J. W.; Hoffmann, R. *J. Am. Chem. Soc.* **1976**, *98*, 1729.
(21) Cockcroft, J. K.; Gibson, V. C.; Howard, J. A. K.; Poole, A. D.; Siemeling, U.; Wilson, C. *J. Chem. Soc., Chem. Commun.* **1992**, 1668.
(22) Schrock, R. R.; Fellmann, J. D. *J. Am. Chem. Soc.* **1978**, *100*, 3359.

(s), 1430 (m), 1380 (m), 1360 (m), 1280 (m), 1100 (w), 1020 (m), 800 (s), 750 (s).

Synthesis of $(C_5H_5)Nb(N\text{-}2,6\text{-}C_6H_3\text{-}i\text{-}Pr_2)(CHDCMe_3)_2$ (6-d_2). $(C_5H_5)Nb(N\text{-}2,6\text{-}C_6H_3\text{-}i\text{-}Pr_2)(CHDCMe_3)_2$ (6-d_2) was prepared by an analogous procedure to that described for $(C_5H_5)Nb(N\text{-}2,6\text{-}C_6H_3\text{-}i\text{-}Pr_2)(CH_2CMe_3)_2$ (6).

X-ray Crystallography. Crystal data for 6 are summarized in Table I. Measurements were made with a Stoe-Siemens four-circle diffractometer and graphite-monochromated Mo Kα radiation (λ = 0.710 73 Å) at 295 K. Unit cell parameters were refined from 2θ values (20–25°) of 32 reflections measured at ±ω to minimize systematic errors. Intensities were measured by an on-line profile fitting method[23] and corrected semiempirically for absorption. Approximately 5% decay in the intensities of the three standard reflections occurred during data collection.

The structure was solved from Patterson and difference syntheses, with blocked-cascade least-squares refinement on F. H atoms were constrained, except for the neopentyl CH_2, for which C–H was restrained to 0.96(1) Å but the orientations of the bonds were allowed to refine freely. All non-H atoms were refined anisotropically. A final difference synthesis showed no features outside +0.41 and −0.23 e Å^{-3}. SHELXTL[24] and locally written computer programs were employed, and atomic scattering factors were taken from ref 25. The weighting scheme was $w^{-1} = \sigma^2(F_o) = \sigma_c^2(F_o) + A_1 + A_2G + A_3G^2 + A_4H + A_5H^2 + A_6GH$, where $G = F_o/F_{max}$ and $H = \sin\theta/\sin\theta_{max}$; the parameters A were derived from analysis of the data.[26] Extinction effects were negligible. The weighted R factor, $R_w = (\sum w\Delta^2/\sum wF_o^2)^{1/2}$.

Acknowledgment. The authors thank B. P. Chemicals for financial support, SERC for a studentship (to D.N.W.) and a research grant (to W.C.), Prof. M. S. Brookhart for helpful discussions, and one of the reviewers for helpful comments. The award (to V.C.G.) of an Edward Frankland Fellowship of the Royal Society of Chemistry is gratefully acknowledged.

Supplementary Material Available: Tables listing the anisotropic thermal parameters and hydrogen atom coordinates with isotropic thermal parameters (11 pages). Ordering information is given on any current masthead page.

OM9301905

(23) Clegg, W. *Acta Crystallogr. A* **1981**, *37*, 22.

(24) Sheldrick, G. M. SHELXTL, an integrated system for solving, refining and displaying crystal structures from diffraction data, Revision 5; University of Göttingen: Germany, 1985; SHELXS86, 1986.

(25) *International Tables for X-ray Crystallography Vol. IV*; Kynoch Press: Birmingham, U.K., 1974; pp 99, 149.

(26) Wang, H.; Robertson, B. E. *Structure and Statistics in Crystallography*; Wilson, A. J. C., Ed.; Adenine Press: New York, 1985; p 125.